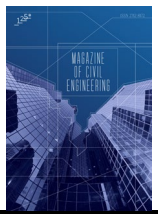

Magazine of Civil Engineering

ISSN 2712-8172

journal homepage: http://engstroy.spbstu.ru/

Research article

UDC 624

DOI: 10.34910/MCE.128.7

Suitability of earthen materials for rammed earth in arid region

E.L. Hasan, M.A. Al-Sharrad ✉

University of Anbar, Ramadi, Iraq

✉ *muayad.alsharrad@uoanbar.edu.iq*

Keywords: earthen materials, rammed earth, sustainable buildings, dynamic adsorption

Abstract. This study investigated the suitability of two engineered earthen materials manufactured by mixing different proportions of sand, silt, and clay for rammed earth constructions under dry conditions. The first mix contained 30 % fine material, whereas the second mix contained 50 % fine material. Test specimens were prepared by static compaction to 4.5, 25, 50, and 100 MPa, equilibrated at relative humidity values of RH = 35 % and RH = 55 % and tested in the lab to characterize plasticity, mechanical, hydric, and thermal behavior. The materials showed a drying shrinkage of no more than 4 %, depending on the initial water content and the unit weight of the material. The results indicated a remarkable increase in materials elastic stiffness and strength of 50 % to 120 % and 10 % to 70 %, respectively, with increasing dry unit weight or compaction energy. The increase in soil suction led to a profound improvement in stiffness and strength, owing to an increase in capillary bonding. In addition, the increase in finer content from 30 % to 50 % significantly enhanced the mechanical behavior. If a minimum compressive strength of 2 MPa is considered, then compacting the earthen material to 50 MPa or greater would provide sufficient strength under the operational humidity RH=55 %. For the mix with 50 % finer content, a compressive strength of almost 5.75 MPa was achieved when the material was compacted to 100 MPa and equalized to RH = 55 %. As relative humidity increased, materials strength decreased where the amount of reduction was found to be inversely proportional to the compaction level and the maximum dry unit weight. The dynamic adsorption behavior was, largely, independent of the amount of compaction energy or finer content. The dynamic adsorption test indicated that the tested materials exchange a considerable amount of moisture with the atmosphere. Compared to traditional brick and concrete blocks, the materials showed good insulation characteristics. It was observed that the increase in finer content yielded slightly higher thermal conductivity values. Overall, the engineered material examined in this work can be potentially used for rammed earth under dry conditions.

Acknowledgments: The authors would like to thank the staff of the soil mechanics lab at the University of Anbar for making lab equipment available for the experimental work of this paper.

Citation: Hasan, E.L., Al-Sharrad, M.A. Suitability of earthen materials for rammed earth in arid region. Magazine of Civil Engineering. 2024. 17(4). Article no. 12807. DOI: 10.34910/MCE.128.7

1. Introduction

The exceptional environmental and energy challenges, particularly in arid regions, have mandated a rebirth of sustainable construction materials and building technologies. One of the major differences between modern and ancient earthen constructions recounts to the ability to engineer a material with preferential properties, such as high strength and excellent durability. Modern earth building techniques have been developed with the objective of optimizing quality control, increasing construction efficiency and reducing labor and material costs.

As a sustainable replacement for conventional building materials like concrete or fired bricks, rammed earth provides a number of advantages. The embodied energy and carbon dioxide footprints of a rammed earth construction can be much lower than that of an identical structure composed of more

traditional materials, such as concrete or masonry [1–3]. In addition, rammed earth buildings outperform traditional buildings in terms of the energy consumed during buildings operation, thanks to the outstanding hygrothermal properties [4, 5]. Moreover, raw rammed earth is eco-friendly and can be fully recyclable.

Despite the numerous advantages of rammed earth regarding sustainability, various limitations restrict its extensive use for constructions. Because of the profound effect of water on the raw rammed earth, the mechanical behavior is always disputable. The admission of moisture into the wall can decrease material strength significantly as a consequence to suction decrease. These concerns have been emerging over the last few decades, see for example [6, 7]. Moreover, rammed earth constructions are quite sensitive to rain and wind erosion and to the effect of aggressive environments, so they frequently need a protection against weathering [8–10].

According to [11], the soil should generally contain a high proportion of sand and gravel, along with silt and just enough clay to serve as a binder, which is also able to provide acceptable hygroscopic and thermal characteristics. According to [12], rammed earth should have a clay fraction of 5 % to 15 %, a silt fraction of 15 % to 30 %, and a sand with fine gravel fraction of 50 % to 70 %.

An interesting statistical analysis of numerous plasticity data on compressed earth blocks (CEB) and adobe was performed in [13]. The analysis indicated significant variation in the liquid limit (LL) and the plastic limit (PL) values for both the CEB and adobe. Nevertheless, according to the researchers, three quarters of the LL values of the CEB material were between 25 % and 45 %, whereas more than half of these values were between 20 % and 40 % for the adobe material. The analysis of the PL values showed that the majority of the PL values were between 15 % and 29 % for both, the CEB and adobe materials.

Having knowledge of the shrinkage factors such as shrinkage limit, linear and volumetric shrinkage is essential to regulate swelling and shrinkage and to avoid serviceability problems such as crack generation and material disintegration in rammed earth buildings. The occurrence of these problems depends on the type and percentage of clay, the materials gradation, and the amount of moisture. Maniatidis and Walker in [11] cited few examples of maximum permissible linear shrinkage values, ranging from 0.05 % to 3 %. According to numerous studies e.g. [14–16], shrinkage and plasticity of the earthen material can be regulated partly by controlling sand proportion.

Durability in the context of earth construction means the ability of the structure and all its elements to withstand the destructive action of weathering and other actions without degradation to the expected service life [11]. The German standard DIN 18945 [17] classified earth bricks with respect to their resistance to water penetration into three classes. The first class should possess sufficient resistance under partial or complete exposure to water without weather protection. The second class should possess sufficient resistance under weather protection condition. The third class is not water resistant and can be specified to only dry applications such as stacked walls. In the present work, the researchers utilized local soils to engineer a sustainable building material favorable for sustainable constructions in arid climate regions with the best use of the passive energy from the atmosphere.

2. Methods and Materials

2.1. Materials

For the present work, local soils brought from two borrow sites near Ramadi city, Iraq, were collected. Two soil types were selected; Soil 1 was a fine material, while Soil 2 was sand. The mineral composition of these soils was examined by performing X-ray fluorescence (XRF) with a Spectro XLab Pro analyzer. Table 1 shows the main minerals comprising these soils.

Table 1. Mineral composition of Soil 1 and Soil 2.

Element	(%) by weight	
	Soil 1	Soil 2
Sodium	1.61	0.09
Magnesium	4.02	0.36
Aluminum	10.61	1.21
Silicon	41.98	71.07
Sulfur	2.39	0.35
Potassium	2.74	0.08
Calcium	15.58	2.57
Titanium	0.83	0.16
Iron	6.00	1.07

2.2. Mixtures and Experimental Procedures

2.2.1. Grain size distribution (GSD)

The grain size distribution was determined according to the ASTM Standard D422 [18] by dry sieving for the material larger than 75 μm and a hydrometer for the material smaller than 75 μm. Soil 1 comprised of 50 % silt and 50 % clay, whereas Soil 2 comprised of 100 % sand.

Neither Soil 1 nor Soil 2 complies with the gradation requirements for earthen building materials suggested in the literature e.g. [19]. Therefore, two new soils were fabricated, namely: Mix 1 with 70 % sand, 15 % silt, and 15 % clay, and Mix 2 with 50 % sand, 25 % silt, and 25 % clay. The gradation curves of Mix 1 and Mix 2 are shown in Fig. 1.

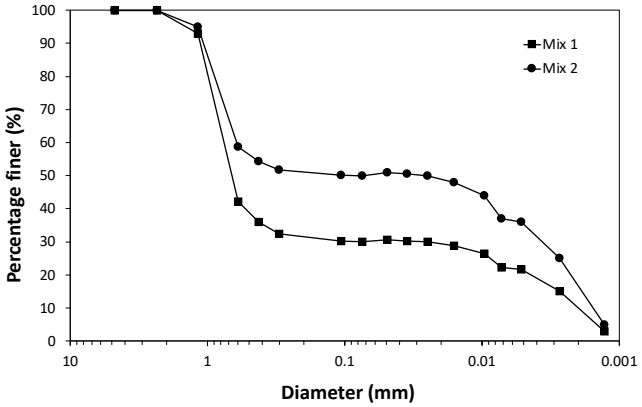

Figure 1. Grain size distribution of Mix 1 and Mix 2.

2.2.2. Plasticity

The liquid limit and plastic limit tests were performed on materials finer than 0.425 mm (sieve No. 40), according to the ASTM Standard D4318 [20]. The plasticity index (PI) was determined as the difference between the liquid limit and the plastic limit of the soil. The shrinkage factors test was performed by the water submersion method of the ASTM Standard D4943 [21] on materials finer than 0.425 mm, taken from Mix 1 and Mix 2. Initially, the samples were mixed thoroughly with water to form a paste with a water content higher than the liquid limit by 10 %. In this test the shrinkage limit (SL), shrinkage ratio (R), volumetric shrinkage (Vs), and linear shrinkage (Ls) are determined. The values of the plasticity factors for Mix 1 and Mix 2 are summarized in Table 2.

Table 2. Plasticity factors of the mixes.

	Liquid limit	Plastic limit	Plasticity index	Shrinkage limit	Shrinkage ratio	Volumetric shrinkage	Linear shrinkage
	LL	PL	PI	SL	R	Vs	Ls
	(%)	(%)	(%)	(%)		(%)	(%)
Mix 1	48.4	23.62	24.8	20.3	1.78	59.7	79.1
Mix 2	54.3	24.2	30.1	14.6	1.82	90.5	82.5

2.2.3. Specimen preparation

Test specimens with 100 mm height and 50 mm in diameter were fabricated by static compaction. A compaction rig was manufactured, as shown schematically in Fig. 2, following the proposal of [22, 23]. This method targets increasing material density, hence providing higher compressive strength, by applying a static compressive force on a laterally confined soil specimen. Specimens were prepared by thoroughly mixing predetermined proportions of the materials in a dry state, then the required amount of water was introduced. Specimen compaction was achieved by pouring one-third of the wet material, each time, inside the mold, then applying constant displacement compression (0.1 mm/min) until a target compressive pressure of 4.5, 25, 50, and 100 MPa was reached. The specimen was unloaded then extruded and taken for weight-volume measurements before being properly stored inside a plastic bag until the next stage. The static compaction pressure 4.5 MPa was relatively small and was only taken as a reference, equivalent to the standard Proctor compaction.

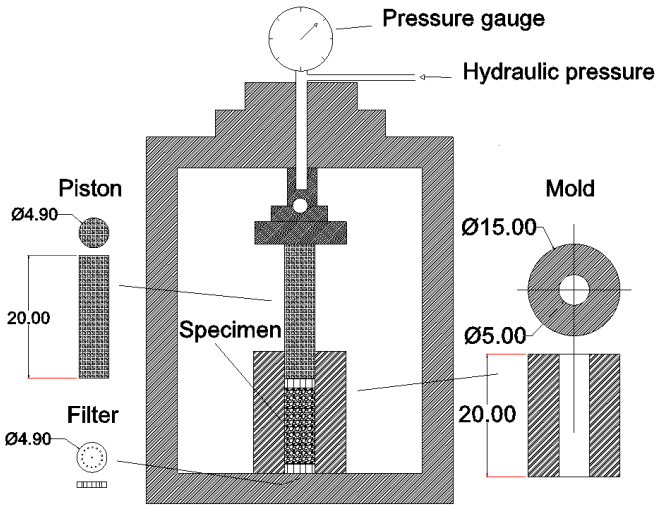

Figure 2. Schematic diagram of the compaction rig.

2.2.4. Compressive strength test

The material stiffness and compressive strength were investigated by performing unconfined compression tests on specimens with different initial unit weight values and moisture states, according to the ASTM Standard D2166 [24]. The test was performed at a constant loading/unloading rate of 1 mm/min. Young's modulus was obtained by performing loading-unloading cycles, between one-ninth and one-third of the estimated compressive strength. The elastic modulus was determined as the average slope of the lines best fitting the unloading branches of these cycles. It is assumed that material behavior is elastoplastic during loading but mainly elastic during unloading. The specimens were subsequently loaded to failure to measure the unconfined compressive strength.

2.2.5. Soil suction test

In this work, the matric and total suctions of the materials were measured indirectly with the filter paper technique, in which the filter paper has a predefined water retention curve. Under vapor equilibrium condition inside a closed system, the soil suction is inferred from the water content of the contact filter paper for matric suction and non-contact filter paper for total suction. Three identical specimens with 20 mm height and 50 mm in diameter were initially prepared at each compaction pressure of the two mixes at the target optimum water content and maximum dry unit weight. Two of these specimens were equalized at a constant temperature of 20 ± 2 °C to a constant mass at relative humidity values of RH = 55 ± 2 % and RH = 35 ± 2 %. These values correspond to the prevailing winter and summer humidity values in Ramadi, respectively. Matric and total suction of these samples were measured with the filter paper technique by the ASTM Standard D5298 [25], using Whatman No. 42 filter papers. Alternatively, for a given constant temperature and relative humidity, the value of total suction can be obtained by using the Kelvin equation [26]:

$$\psi = -\frac{RT}{V_m}\ln\left(RH\right), \tag{1}$$

where R is the universal gas constant (8.31 J mol^{-1} K^{-1}), T is the absolute temperature (K) and V_m is the molar volume of water (18*10^{-6} m^3/mol). The containers were kept closed for 10 days in order to achieve vapor pressure equilibrium of the water in the filter papers, the specimen and the air inside the container.

2.2.6. Moisture buffering

The absorptive behavior of the material was evaluated by measuring the moisture buffering value (MBV) following the NORDTEST project method described in [27]. The practical MBV is calculated as follows:

$$MBV_{practical} = \frac{\Delta m}{S\Delta\%RH}, \tag{2}$$

where $MBV_{practical}$ quantifies the amount of moisture $\left(\Delta m\right)$ gained or released per exposed surface area (S) over a given time interval as a result of a variety of relative humidity $\left(\Delta\%RH\right)$. For each mix, four

samples with 100 mm height and 50 mm in diameter were prepared at the optimum water content and dry unit weight corresponding to 4.5, 25, 50, and 100 MPa compaction pressure. These specimens were then conditioned inside a humidity room to the same relative humidity of RH=55 %. The specimens were mounted in an upright position in such a manner that the top and the curved faces were the only ones exposed to RH variation. Subsequently, the samples were subjected to a step cyclic increase/decrease of RH between 75 ± 2 % and 50 ± 2 % until a virtually constant mass of water was absorbed/released over the last few cycles. The step increase/decrease was performed every 12 hours. Meanwhile, the specimen weight was frequently recorded.

2.2.7. Thermal conductivity

The steady-state coefficient of thermal conductivity of the earthen material was tested using WL373 thermal conductivity meter, as shown in Fig. 3. Soil specimens with 30 mm height and 21 mm in diameter were compacted to predefined moisture and unit weight values inside a HDPE tube, which was placed inside the compaction mold. A set of three specimens were prepared at the maximum dry unit weight of each compaction pressure. Then two of each set were equalized at a relative humidity of RH = 55 ± 2 % and RH = 35 ± 2 %, under a constant temperature of 20 ± 2 °C. The test specimen is mounted between a heat source and a heat sink. A steady-state heat flux (Q) was applied, while the temperature drop across the specimen (ΔT) was monitored and measured by thermocouples installed close to the specimen faces. The coefficient of thermal conductivity (k) was calculated under steady-state temperature distribution as [28]:

$$k = \frac{QL}{A\Delta T}, \tag{4}$$

where L and A are the length and the cross-sectional area of the sample, respectively.

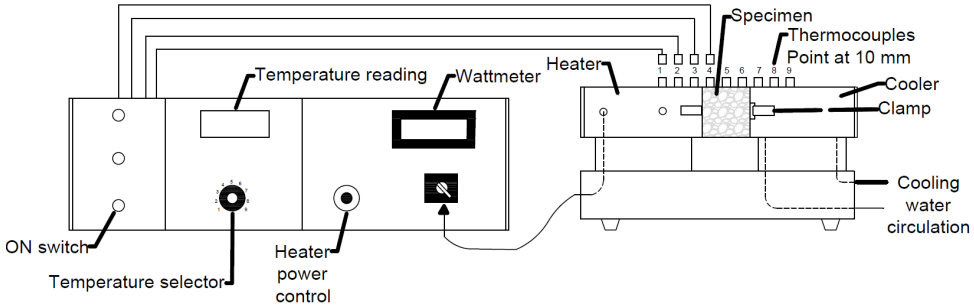

Figure 3. Thermal conductivity meter model WL373.

3. Results and Discussion

3.1. Compaction Characteristics

The compaction curves of Mix 1 and Mix 2 for 4.5, 25, 50, and 100 MPa compaction pressures are shown in Fig. 4. The maximum dry unit weight increased and the optimum water content decreased with increasing compaction energy. For Mix 1, the maximum dry unit weight increased from 19.94 kN/m^3 to 21.91 kN/m^3, while the corresponding optimum moisture content decreased from 10 % to 4.2 % when compaction pressure increased from 4.5 to 100 MPa. Similarly, for Mix 2, the maximum dry unit weight increased from 19.02 kN/m^3 to 21.51 kN/m^3, while the corresponding optimum moisture content decreased from 12.5 % to 5.8 %.

The variation of dry unit weight with compaction energy, as shown in Fig. 5, follows a nonlinear pattern, in which the former tends toward an ultimate virtual value corresponding to zero porosity. Therefore, the higher the compaction pressure, effectively up to 75 MPa, the lower the porosity. Mix 2 always showed lower unit weights compared to Mix 1, despite its high finer content. This is probably attributed to the higher suction values attained by Mix 2 specimens. In addition, the corresponding decrease in porosity was found to be from 22.1 % to 14.4 % and from 25.7 % to 16.0 % for Mix 1 and Mix 2, respectively. These observations are in good agreement with those reported by many researchers, e.g. [22, 29].

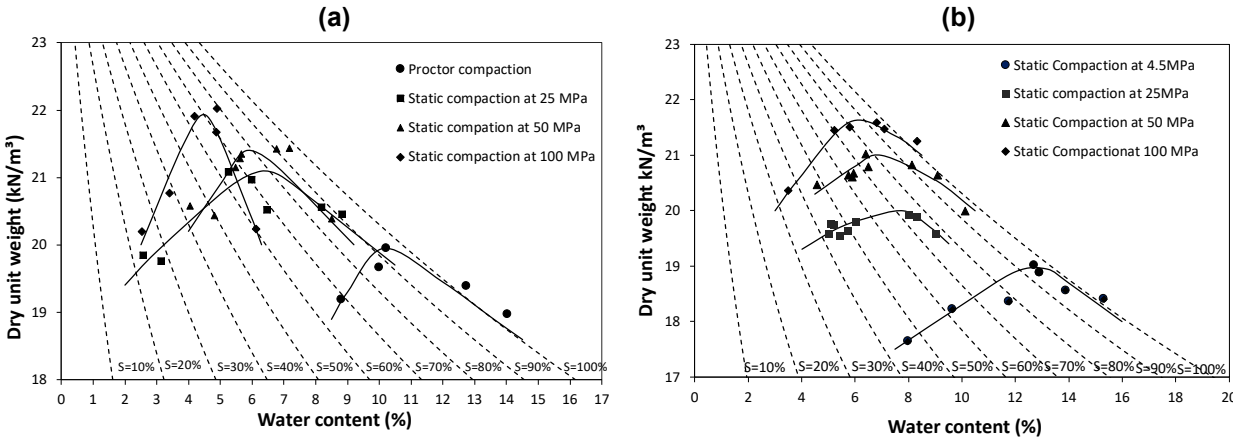

Figure 4. Compaction characteristics for: (a) Mix 1, (b) Mix 2.

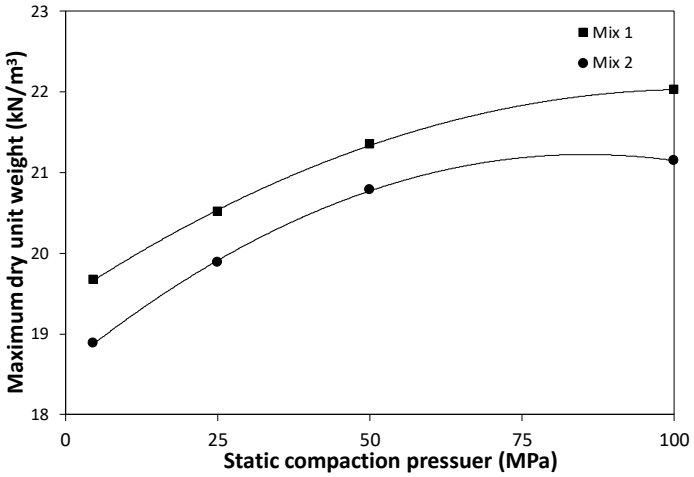

Figure 5. Variation of as-compacted maximum dry unit weight with compaction pressure.

3.2. Moisture Equalization

The moisture equalization was performed under the constant temperature 20 ± 2 °C and the relative humidity RH = 55 ± 2 % and RH = 35 ± 2 %. Over the equalization period, specimen's water content was decaying exponentially. Moisture equilibrium was practically achieved, under a given constant RH, when the mass of the specimens varied by less than 0.1 % during a minimum of one week. On average, moisture equilibrium was achieved after at least one month. In theory, the rate of evaporation of pore water is affected by the difference in relative humidity of the pore air and that of the adjacent air outside the specimen. In principle, the drying process continues until a particular vapor pressure satisfying equilibrium condition is achieved. Fig. 6 illustrates that a modest increase in the dry unit weight took place due to moisture equalization of Mix 1 and Mix 2 specimens originally compacted at the optimum moisture content to 4.5, 25, 50, and 100 MPa.

The amount of shrinkage that occurs due to drying from the as-compacted state to the state at RH=35 % was calculated based on the specimen volume before and after the equalization. A general trend emerged that the higher the initial water content, the higher the drying shrinkage will be. Conversely, the higher the dry unit weight, the lower the drying shrinkage will be. The maximum amount of drying shrinkage, which was nearly 4 %, is considerably lower than the volumetric shrinkage (see Table 2). Thanks to the compaction technique that allows production of dense material at rather low optimum moisture content (4–7 %). By the end of the equalization stage, no shrinkage cracks or discontinuities were observed in the specimens. This promotes the selected material for the next level of the investigation, as illustrated in the following sections.

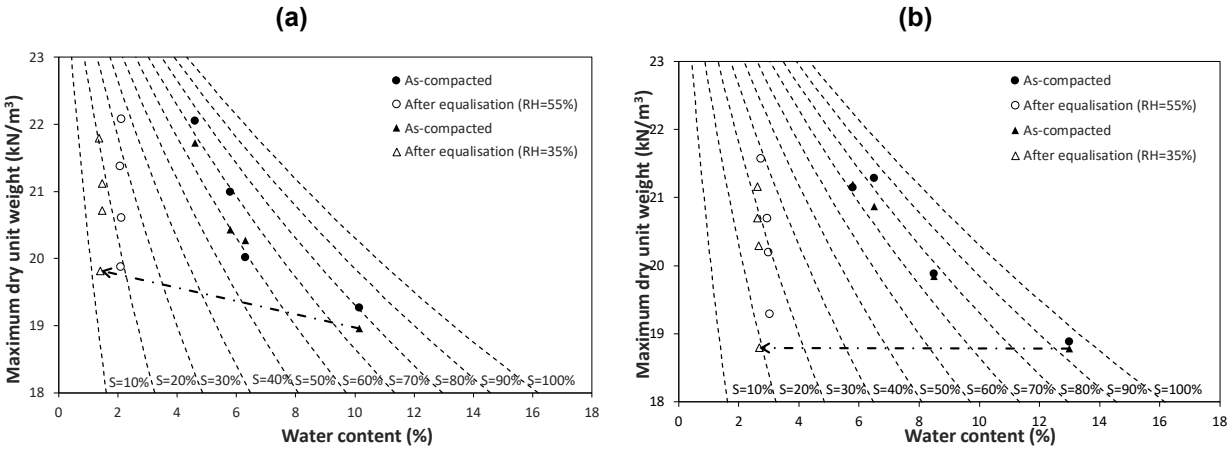

Figure 6. Changes in dry unit weight and water content during equalization for: (a) Mix 1, (b) Mix 2.

3.3. Soil Suction

Fig. 7 presents the variation of total and matric suction with degree of saturation, measured after achieving moisture equilibrium at RH=55 % and RH=35 % as well as at the as-compacted states. Both total and matric suction values were progressively increasing with saturation decreasing. For a given water content, Mix 2 expectedly showed higher suction values than Mix 1, owing to the higher clay content, which in turn resulted in smaller pore sizes and higher adsorption. It appears that the moisture equilibrium brought the saturation and the suction to a residual state. At the residual water content region, most likely at water contents less than 2 %, the residual total and matric suction became the same. This is anticipated where the capillary effect ceases and the available water forms a thin layer surrounding the solid particles. The variation of suction with saturation, i.e. with RH, has several consequences on earthen material strength and the hygrothermal response, as will be explained later in this paper. It was noticed that the higher the dry unit weight of the soil, the more slowly the saturation declines when suction is increased (i.e. when the RH was set to 55 % and 35 %). The soil specimen's smaller, interconnecting pores most likely caused this.

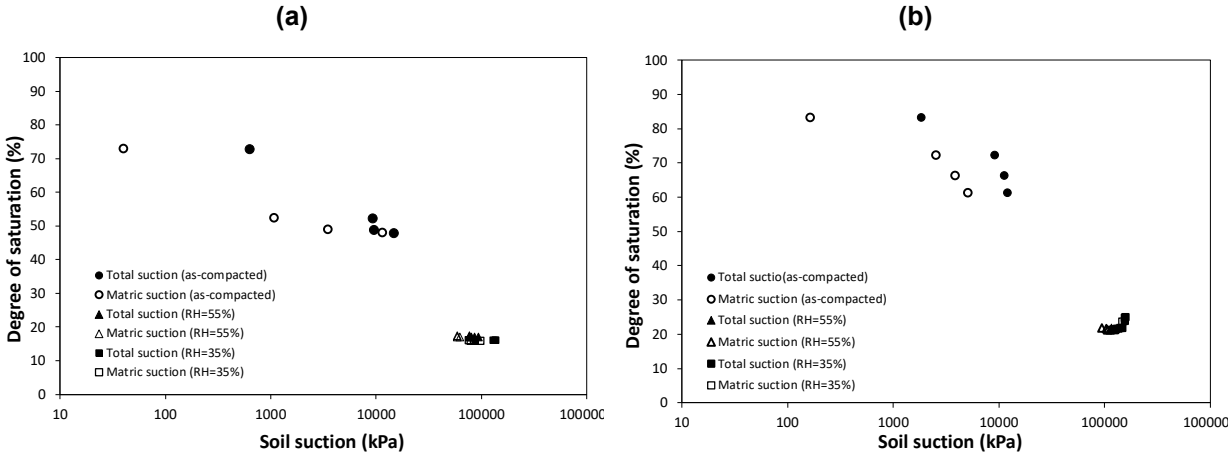

Figure 7. Variation of total and matric suction with degree of saturation for: (a) Mix 1, (b) Mix 2.

3.4. Mechanical Behavior

Three identical specimens initially compacted to 4.5, 25, 50, and 100 MPa for each mix. The main objective was to determine the effect of the compaction pressure (hence the dry unit weight), moisture variation, and finer content, on the stiffness and strength of the unstabilized earth. To imitate the effect of materials moisture variation triggered by ambient humidity variation, two of each three identical compacted specimens were brought to moisture equilibrium at RH = 55 % and RH = 35 % inside the humidity room. Fig. 8 presents typical stress-strain response for specimens compacted to 100 MPa. Fig. 9 captures the effect of dry unit weight increase on earthen material stiffness and compressive strength for Mix 2. These material variables increased substantially, in a nonlinear fashion, with increasing dry unit weight as a result of frictional resistance increase.

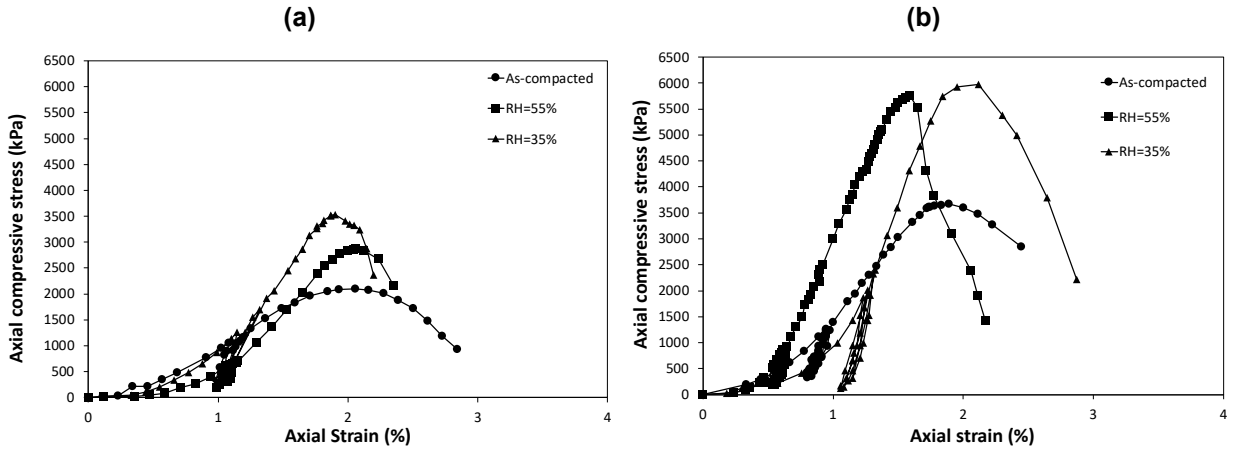

Figure 8. Typical stress-strain behavior for specimens compacted at 100 MPa: (a) Mix 1, (b) Mix 2.

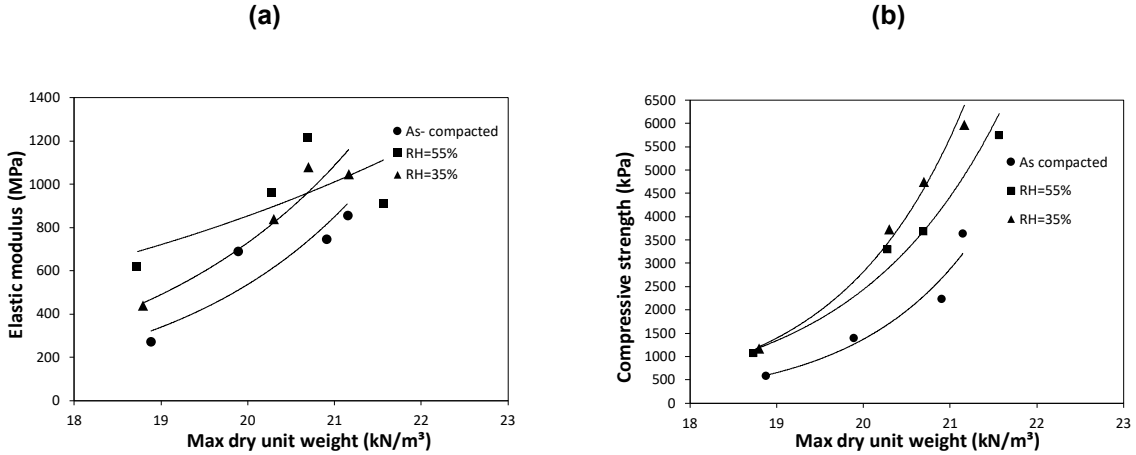

Figure 9. Variation of Young's modulus and the compressive strength with dry unit weight for Mix 2.

3.5. Effect of the Relative Humidity Variation

The effect of relative humidity variation, expressed in terms of total suction, on the stiffness and compressive strength of Mix 2 specimens is shown in Fig. 10. The total suction appears to have a profound effect on the stiffness and strength of the earthen material. A similar observation can be found in [30]. The increase of suction produced a remarkable increase in Young's modulus and compressive strength. For instance, compressive strength of specimens compacted to 50 MPa increased from just about 1400 kPa to slightly less than 2600 kPa for Mix 1 and from 2200 kPa to 4750 kPa for Mix 2, over suction variation from the as-compacted state to that corresponding to RH=35 %. As the earthen material dries, capillary suction increases leading to an increase in stiffness and strength.

Raw earth is characterized by the presence of meniscus water bridges between particles, which generate capillary bonding thereby increasing the overall strength and stiffness of the material. In other words, the mechanical properties of compacted earth improve, as degree of saturation decreases with decreasing ambient humidity. At the same time, the material becomes more brittle as the ability of the material to undergo substantial plastic straining before failure decreases with drying, see for example Fig. 8.

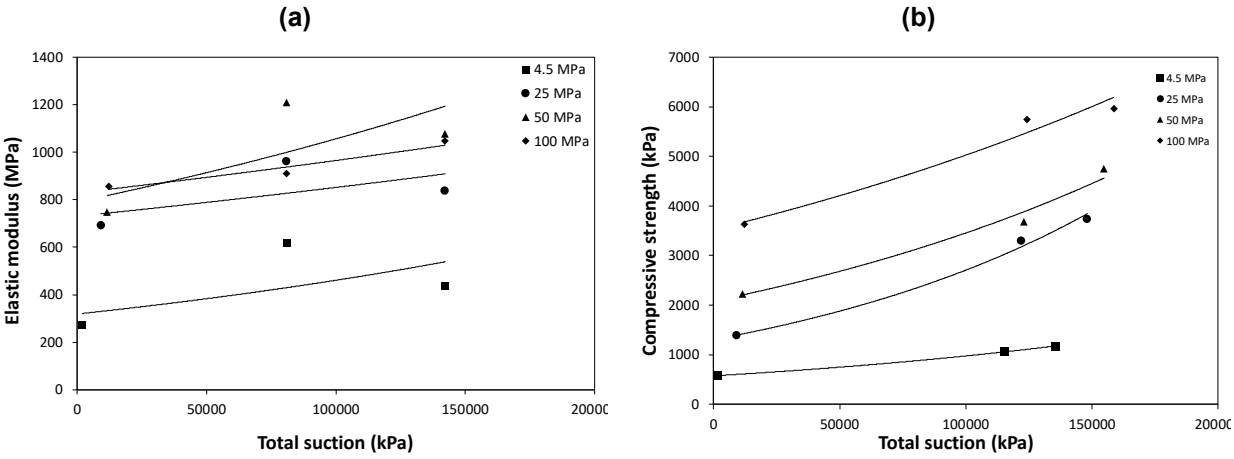

Figure 10. Variation of strength and Young's modulus with suction for Mix 2.

Results analysis indicated that Mix 1 could provide a minimum compressive strength of 1300 to 2900 kPa and provide a maximum compressive strength of 2300 to 3500 kPa when the material statically compacted to pressure level between 25 and 100 MPa, as shown in Table 3. Instead, Mix 2 could provide a minimum compressive strength of 3300 to 5750 kPa and provide a maximum compressive strength of 3700 to 6000 kPa when the material statically compacted between 25 and 100 MPa. The minimum and the maximum figures above correspond to the RH = 55 % and RH = 35 %, respectively. For a given compaction condition, the compressive strength decreases with increase in relative humidity as per Table 3. The reduction in strength appears to show a dependency on the compaction level where specimens compacted at 100 MPa preserved more strength upon wetting than those compacted at 50 and 25 MPa. That suggests that material mechanical behavior is more controlled by variables, such as pore size and pore size distribution, than by the effect of suction.

Table 3. Reduction in strength produced by an increase of RH from 35 % to 55 %.

Mix	Compaction pressure (MPa)	Compressive strength (kPa)		Reduction in strength (%)
		RH = 35 %	RH = 55 %	
Mix 1	25	2300	1300	43
	50	2600	2000	23
	100	3500	2900	17
Mix 2	25	3700	3300	11
	50	4750	3700	22
	100	6000	5750	4

3.6. Moisture Buffering

Each specimen was subjected to seven cycles of a relative humidity step change between RH = 50 % and RH = 75 %. The moisture buffering value (MBV) was calculated from Equation 1, see a typical variation of the MBV in Fig. 14 for Mix 2. During the first few cycles, the MBV tended to be greater for moisture absorption than for moisture release. The last few cycles indicated that the tested material has a moisture buffering values of about 1.50 and 1.55 (g/ (m^2%RH)) for Mix 1 and Mix 2, respectively. The increase in finer content does not appear to improve the moisture exchange between the material and the atmosphere. Further investigation is therefore required on the materials sorption capacity and materials vapor permeability. It can be seen that the hygroscopic behavior of the specimens is essentially the same regardless of the differences in initial unit weight.

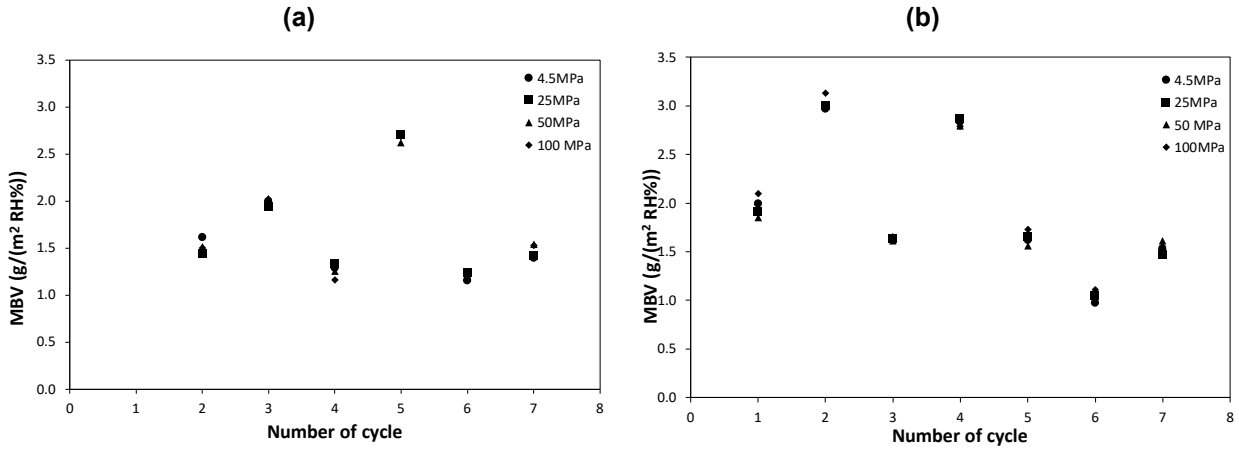

Figure 11. Typical moisture buffering variation for Mix 2 for: (a) moisture adsorption, (b) moisture release.

3.7. Thermal conductivity

Fig. 12 shows typical variation of the coefficient of thermal conductivity (k) with bulk unit weight and degree of saturation for Mix 2. Inspection of this figure suggests that k generally decreased with increasing material's bulk unit weight but tend to increase slightly with increasing saturation. As saturation increases, pore air is gradually replaced by water, which possesses significantly higher thermal conductivity. It is believed that under a residual state, which may occur at saturation degrees less than 15 % for Mix 1 and 30 % for Mix 2, the water mainly exists as a thin film surrounding the particles. This residual water is not expected to contribute much to the thermal conductivity. At higher saturation degrees, the water menisci are formed at the inter-particles contacts, leading to an increase in the thermal conductivity. Over the examined range of unit weight and degree of saturation values, the thermal conductivity *k* varied from 1.10 to 1.35 W/(m.K) for Mix 1 and from 1.2 to 1.3 W/(m.K) for Mix 2. These figures of the current earthen material are comparable to those of other construction materials, such as adobe blocks and fired bricks, see [31].

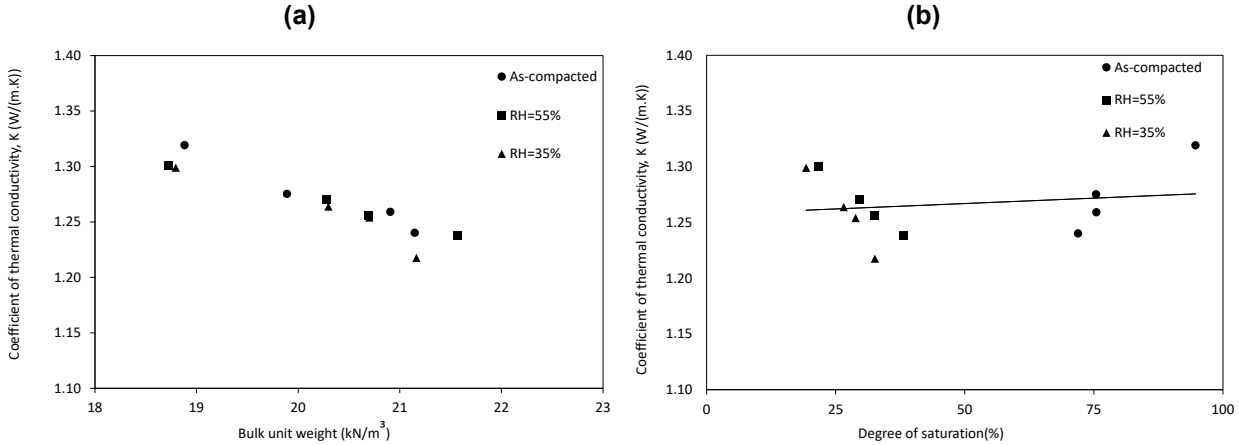

Figure 12. Variation of the thermal conductivity of Mix 2 with: (a) bulk unit weight, (b) degree of saturation.

3.8. Microstructural Characteristics

Fig. 13 shows SEM images taken at 7000× magnification of samples taken from Mix 1 and Mix 2, compacted to 25 MPa or to 100 MPa. Comparison of Fig. 13a and 13b indicates that the Mix 1 sample exhibited larger pore sizes compared to the Mix 2 sample. These pores became very small for the compaction pressure 100 MPa, as can be seen in Fig. 13c and 13d. In addition, aggregations of fine particles can be observed very clearly on the samples compacted to 25 MPa. These aggregations are an inherited feature of compacted materials, formed when water is introduced during the compaction process. A dual-porosity structure, characterized by macro pores between the aggregates and micro pores between the particles, can be observed. As the compaction pressure proceeds to100 MPa, the macro pores became progressively smaller.

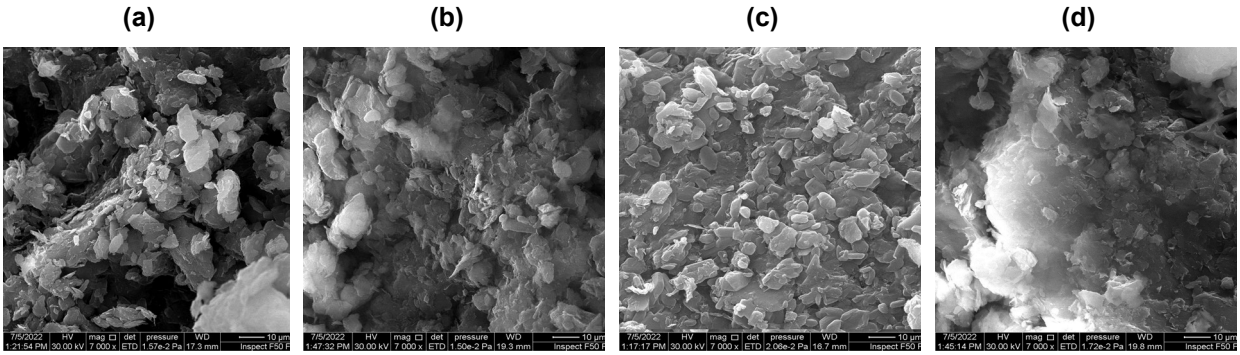

Figure 13. SEM images of: (a) Mix 1, 25 MPa; (b) Mix 2, 25 MPa; (c) Mix 1, 100 MPa; (d) Mix 2, 100 MPa.

3.9. Effect of Fine Content on the Earthen Material Behavior

A quantitative comparison on the effect of increasing finer content on soil suction, stiffness, compressive strength, moisture buffering, and thermal conductivity is presented in Fig. 14–18. Structurally, Mix 2 outperforms Mix 1 with respect to stiffness, provided that failure occurred at rather the same strain level (about 1–2 %). Mix 2 showed also a superior response, with respect to compressive strength, compared to Mix 1 at almost all the compaction pressure levels. The compressive strength increased remarkably by 60–150 % as the finer content increased from 30 % to 50 %. This improvement cause the increase of binder content and the increase of capillary suction, as shown in Fig.16. Mix 2, unlike Mix 1, showed a marginal increase in the moisture buffering value with increasing compaction pressure. In terms of thermal conductivity, Mix 2 tended to generally show marginally higher k values than Mix 1, with few exceptions, as shown in Fig. 18. These comparisons suggest that increasing finer content to certain levels can improve earthen material behavior, particularly stiffness and strength.

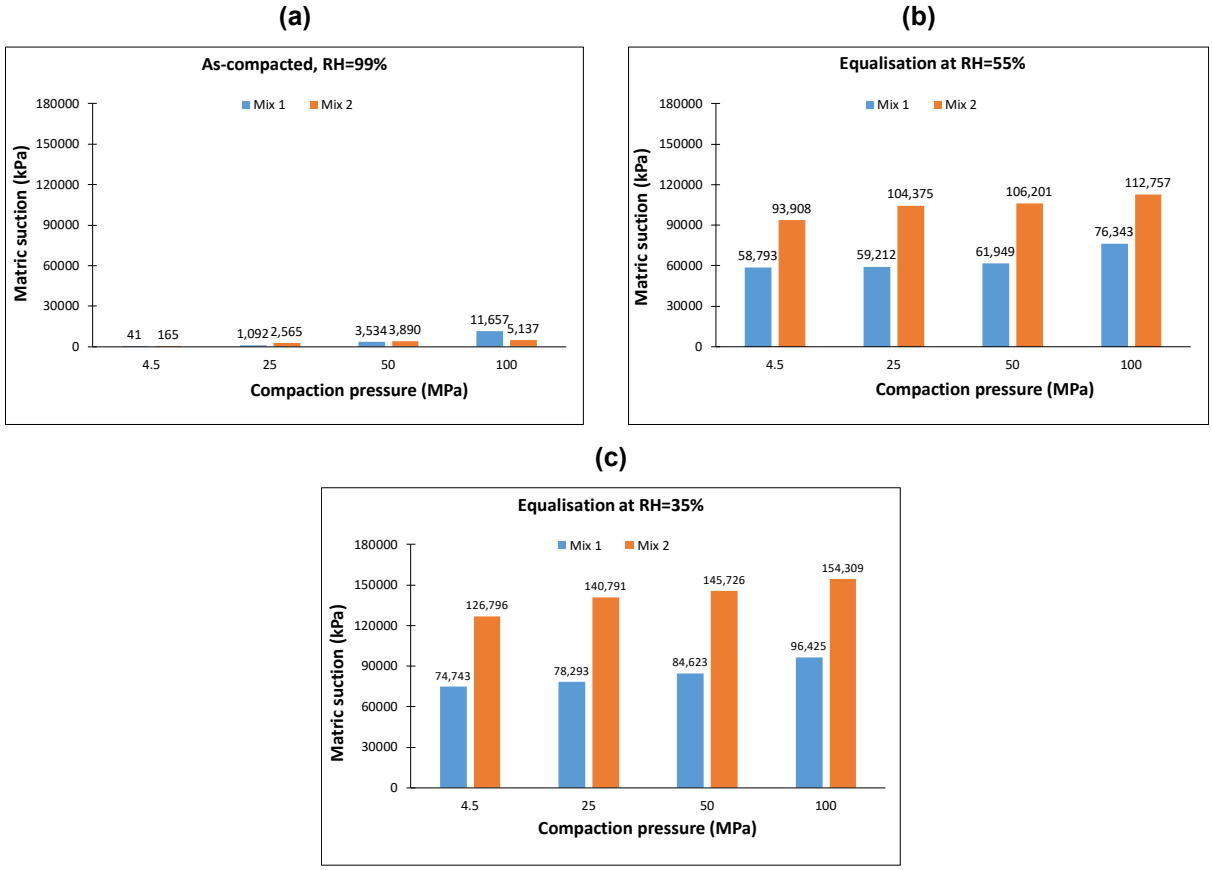

Figure 14. Comparison of matric suction values for Mix 1 and Mix 2: (a) at as-compacted state, (b) at RH = 55 %, (c) at RH = 35 %.

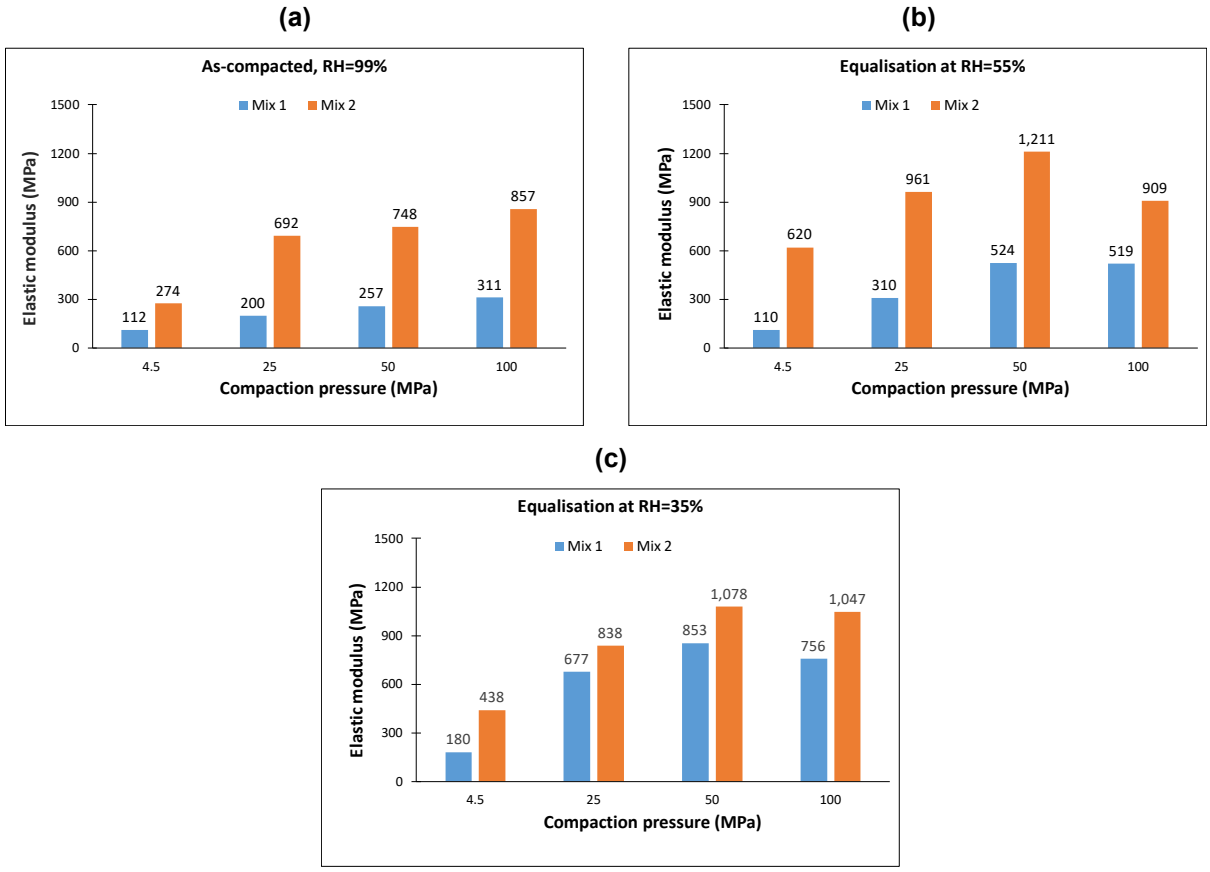

Figure 15. Comparison of Young's modulus values for Mix 1 and Mix 2: (a) at as-compacted state, (b) at RH = 55 %, (c) at RH = 35 %.

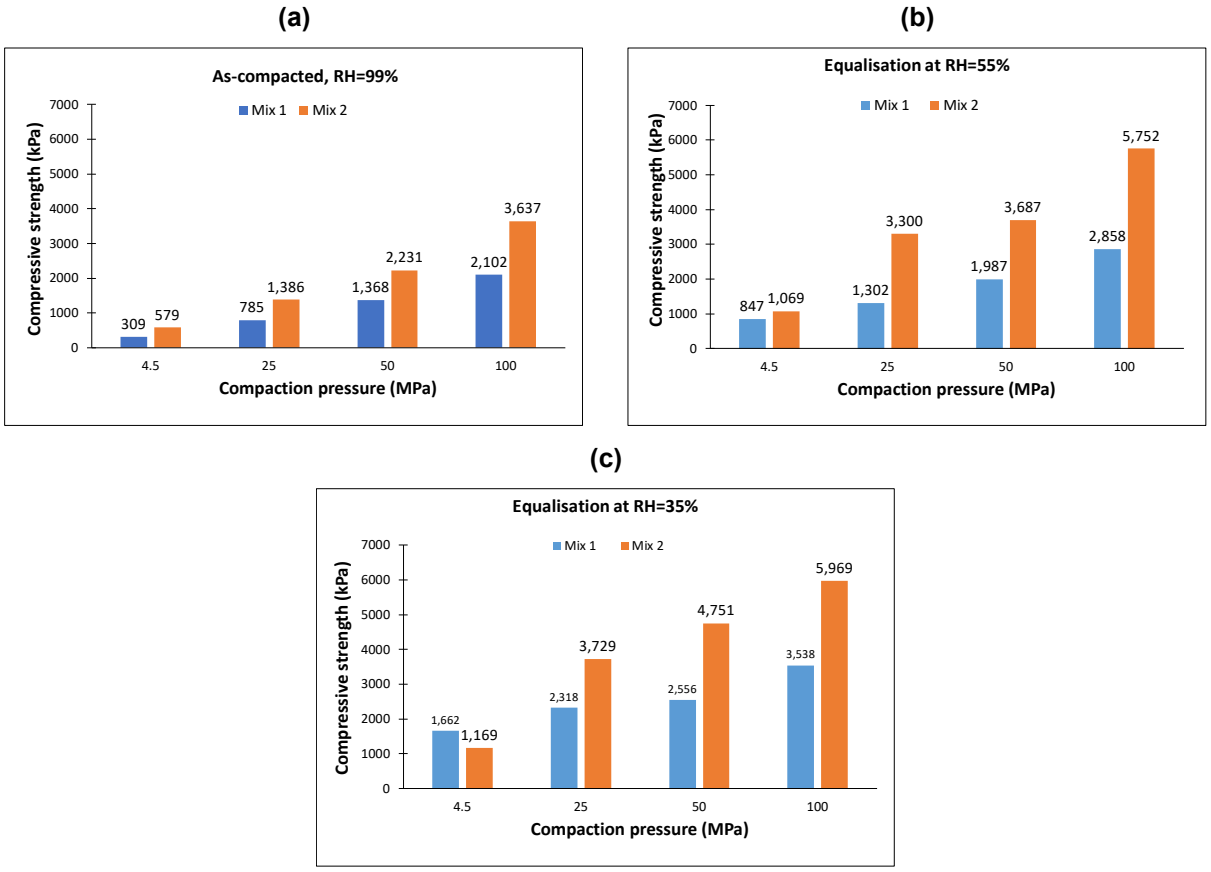

Figure 16. Comparison of compressive strength values for Mix 1 and Mix 2: (a) at as-compacted state, (b) at RH = 55 %, (c) at RH = 35 %.

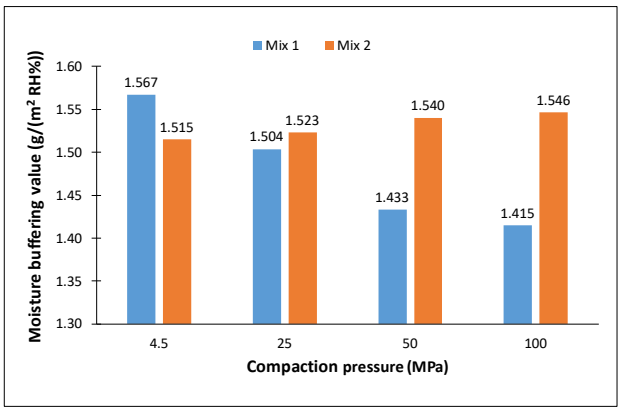

Figure 17. Comparison of moisture buffering values for Mix 1 and Mix 2.

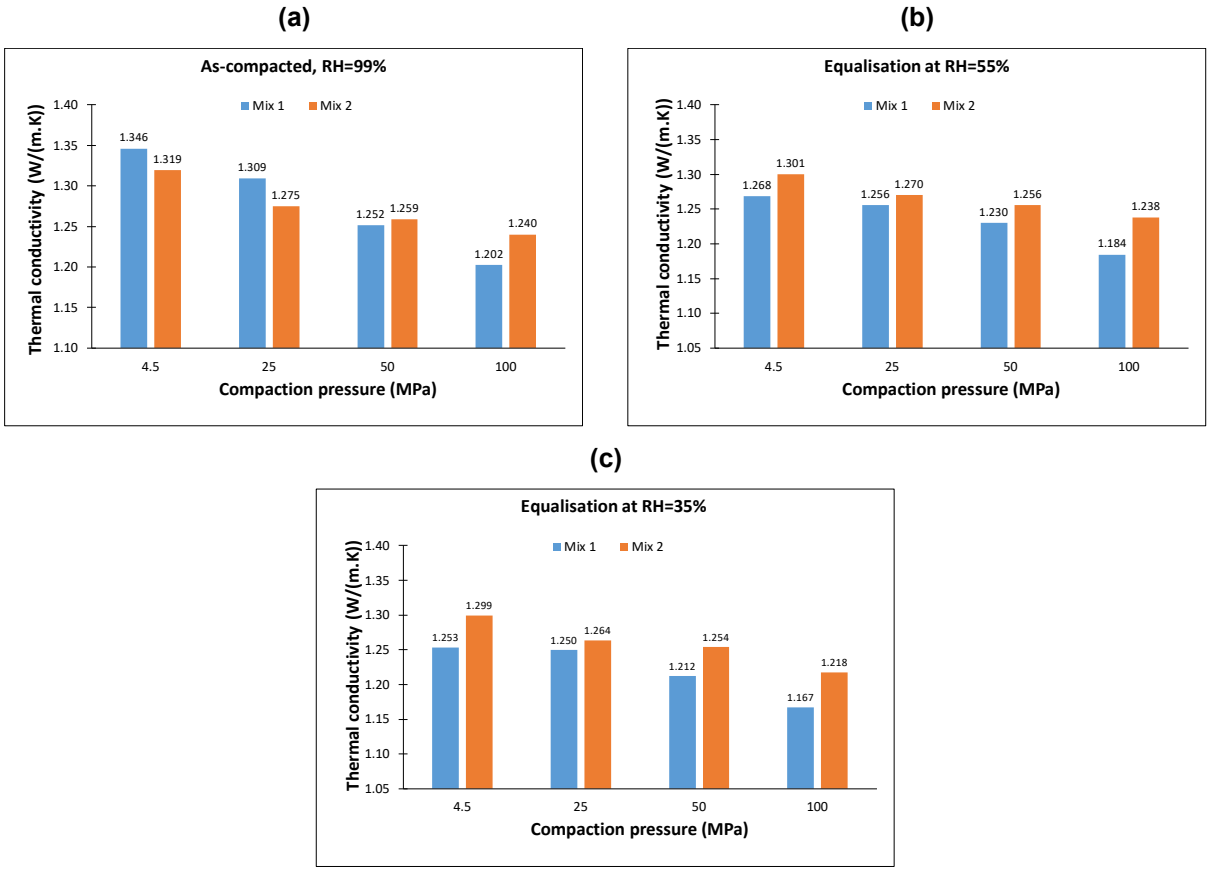

Figure 18. Comparison of thermal conductivity coefficient values for Mix 1 and Mix 2: (a) at as-compacted state, (b) at RH = 55 %, (c) at RH = 35 %.

4. Conclusions

The current work studied suitability of two raw earthen materials for unstabilized rammed earth buildings, based on their physical properties. Two mixes made of different proportions of sand, silt, and clay were prepared. A set of laboratory tests was performed on specimens compacted statically to 4.5, 25, 50, and 100 MPa to characterize mechanical, hydric, and thermal behavior of these materials. Upon drying from the as-compacted moisture to the moisture states corresponding to RH=35 %, the material showed a drying shrinkage between 0 % and 4 %, depending on the initial water content and the unit weight of the material. In addition, the compacted materials were found free of shrinkage cracks even under a completely dry state.

With increasing dry unit weight, frictional resistance increased and produced a noticeable increase in materials stiffness and strength. Likewise, with increasing soil suction, i.e. when relative humidity decreases, a remarkable increase in the elastic modulus and compressive strength was observed. The stiffness and strength were found to increase with increasing finer content from 30 % to 50 %. If a threshold compressive strength of 2 MPa is considered, then compacting the earthen material to at least 50 MPa

would provide sufficient strength under the operational high humidity RH = 55 %. A significant gain in strength was achieved by increasing the compaction pressure to 100 MPa. For example, the mixture with 50 % finer content, achieved a compressive strength of almost 6 MPa when compacted to 100 MPa. In addition, the reduction in strength due to relative humidity increase appeared to show a dependency on the compaction level where specimens compacted at 100 MPa preserved more strength upon wetting than those compacted at 50 and 25 MPa.

Interestingly, the dynamic adsorption behavior appeared to be rather independent of the mount of compaction energy or finer content. The increase in finer content showed a minor increase in the dynamic adsorption with increasing compaction pressure. Nevertheless, the moisture buffering test indicated that both materials exchange sufficient amount of moisture with the atmosphere. On the thermal conductivity front, the increase in finer content yielded slightly higher thermal conductivity values. Despite that, the materials exhibited good insulation characteristics, compared to traditional brick and concrete blocks. Finally, it is concluded that the engineered material examined in this work can be potentially used for rammed earth for dry applications. When comparing both the mixtures, Mix 2 is considered to be preferable due to its higher strength and stiffness, compared to Mix 1.

References

1. Morel, J.C., Mesbah, A., Oggero, M., Walker, P. Building houses with local materials: means to drastically reduce the environmental impact of construction. Building and Environment. 2001. 36(10). Pp. 1119–1126. DOI: 10.1016/S0360-1323(00)00054-8
2. Venkatarama Reddy, B.V., Jagadish, K.S. Embodied energy of common and alternative building materials and technologies. Energy and Buildings. 2003. 35(2). Pp. 129–37. DOI: 10.1016/S0378-7788(01)00141-4
3. Ciancio, D., Boulter, M. Stabilised rammed earth: a case study in Western Australia. Proceedings of the Institution of Civil Engineers – Engineering Sustainability. 2012. 165(2). Pp. 141–154. DOI: 10.1680/ensu.10.00003
4. Beckett, C., Augarde, C. The Effect of Relative Humidity and Temperature on the Unconfined Compressive Strength of Rammed Earth. Unsaturated Soils: Research and Applications. Berlin, Heidelberg: Springer. 2012. Pp. 287–292. DOI: 10.1007/978-3-642-31116-1_39
5. Gallipoli, D., Bruno, A.W., Perlot, C., Salmon, N. Raw earth construction: Is there a role for unsaturated soil mechanics? Unsaturated Soils: Research & Applications. Sydney: CRC Press. 2014. Pp. 55–62. DOI: 10.1201/b17034
6. Jaquin, P.A., Augarde, C.E., Gallipoli, D., Toll, D.G. The strength of unstabilised rammed earth materials. Géotechnique. 2009. 59(5). Pp. 487–490. DOI: 10.1680/geot.2007.00129
7. Bui, T.T., Bui, Q.-B., Limam, A., Maximilien, S. Failure of rammed earth walls: From observations to quantifications. Construction and Building Materials. 2014. 51. Pp. 295–302. DOI: 10.1016/j.conbuildmat.2013.10.053
8. Ghasemalizadeh, S., Toufigh, V. Durability of rammed earth materials. International Journal of Geomechanics. 2020. 20(11). DOI: 10.1061/(ASCE)GM.1943-5622.0001829
9. Arrigoni, A., Beckett, C., Ciancio, D., Dotelli, G. Life cycle analysis of environmental impact vs. durability of stabilised rammed earth. Construction and Building Materials. 2017. 142. Pp. 128–136. DOI: 10.1016/j.conbuildmat.2017.03.066
10. Luo, Y., Yang, M., Ni, P., Peng, X., Yuan, X. Degradation of rammed earth under wind-driven rain: The case of Fujian Tulou, China. Construction and Building Materials. 2020. 261. Article no. 119989. DOI: 10.1016/j.conbuildmat.2020.119989
11. Maniatidis, V., Walker, P. A Review of rammed earth construction. 2003. Paper presented at DTI Project Report, Bath. [Online]. URL: https://people.bath.ac.uk/abspw/rammedearth/review.pdf (accessed: 28.05.2024).
12. Standard SADC ZW HS 983: Rammed earth structures – Code of practice. [Online]. URL: https://www.rammedearthconsulting.com/library/african-rammed-earth-harmonised-standard-en.pdf (accessed: 28.05.2024)
13. Aubert, J.E., Faria, P., Maillard, P., Ouedraogo, K.A.J., Ouellet-Plamondon, C., Prud'homme, E. Characterization of Earth Used in Earth Construction Materials. Testing and Characterisation of Earth-based Building Materials and Elements. RILEM State-of-the-Art Reports. 35. Springer, Cham, 2022. Pp. 17–81. DOI: 10.1007/978-3-030-83297-1_2
14. Walker, P.J. Strength, durability and shrinkage characteristics of cement stabilised soil blocks. Cement and Concrete Composites. 1995. 17(4). Pp. 301–310. DOI: 10.1016/0958-9465(95)00019-9
15. Walker, P. Bond characteristics of earth block masonry. Journal of Materials in Civil Engineering. 1999. 11(3). Pp. 249–256. DOI: 10.1061/(ASCE)0899-1561(1999)11:3(249)
16. Guettala, A., Mezghiche, B., Chebili, R., Houari, H. Durability of lime stabilised earth blocks. Challenges of Concrete Construction. 2002. 5. Pp. 645–654. DOI: 10.1680/scc.31777.0064
17. Deutsches Institut für Normung (DIN). Earth blocks – Terms and definitions, requirements, test methods. DIN 18945. 2013.
18. American Society of Testing and Materials (ASTM). Standard test method for particle-size analysis of soils. ASTM D422. West Conshohocken PA: ASTM International, 2007. 8 p.
19. Ciancio, D., Jaquin, P., Walker, P. Advances on the assessment of soil suitability for rammed earth. Construction and Building Materials. 2013. 42. Pp. 40–47. DOI: 10.1016/j.conbuildmat.2012.12.049
20. American Society of Testing and Materials (ASTM). Standard test methods for liquid limit, plastic limit, and plasticity index of soils. ASTM D4318. West Conshohocken PA: ASTM International, 2017. 20 p.
21. American Society of Testing and Materials (ASTM). Standard test method for shrinkage factors of cohesive soils by the water submersion method. ASTM D4943. West Conshohocken PA: ASTM International, 2018. 7 p.
22. Bruno, A.W., Gallipoli, D., Perlot, C., Mendes, J. Effect of very high compaction pressures on the physical and mechanical properties of earthen materials. E3S Web of Conferences. 2016. 9. Article no. 14004. DOI: 10.1051/e3sconf/20160914004
23. Gallipoli, D., Bruno, A.W., Perlot, C., Mendes, J. A geotechnical perspective of raw earth building. Acta Geotechnica. 2017. 12. Pp. 463–478. DOI: 10.1007/s11440-016-0521-1

24. American Society of Testing and Materials (ASTM). Standard test method for unconfined compressive strength of cohesive soil. ASTM D2166. West Conshohocken PA: ASTM International, 2016. 6 p.
25. American Society of Testing and Materials (ASTM). Standard test method for measurement of soil potential (suction) using filter paper. ASTM D5298. West Conshohocken PA: ASTM International, 2016. 6 p.
26. Likos, W.J., Lu, N. Filter Paper Technique for Measuring Total Soil Suction. Transportation Research Record: Journal of the Transportation Research Board. 2002. 1786(1). Pp. 120–128. DOI: 10.3141/1786-14
27. Rode, C. et al. Moisture Buffering of Building Materials. Technical University of Denmark, Department of Civil Engineering. 2005. BYG Report No. R-127. [Online]. URL: https://backend.orbit.dtu.dk/ws/portalfiles/portal/2415500/byg-r126.pdf (accessed: 28.05.2024)
28. Zhao, D., Qian, X., Gu, X., Jajja, S.A., Yang, R. Measurement techniques for thermal conductivity and interfacial thermal conductance of bulk and thin film materials. Journal of Electronic Packaging. 2016. 138(4). Article no. 040802. DOI: 10.1115/1.4034605
29. Kouakou, C.H., Morel, J.C. Strength and elasto-plastic properties of non-industrial building materials manufactured with clay as a natural binder. Applied Clay Science. 2009. 44(1–2). Pp. 27–34. DOI: 10.1016/j.clay.2008.12.019
30. Xu, L., Wong, K.K., Fabbri, A., Champiré, F., Branque, D. Loading-unloading shear behavior of rammed earth upon varying clay content and relative humidity conditions. Soils and Foundations. 2018. 58(4). Pp. 1001–15. DOI: 10.1016/j.sandf.2018.05.005
31. Bruno, A.W., Gallipoli, D., Perlot, C., Kallel, H. Thermal performance of fired and unfired earth bricks walls. Journal of Building Engineering. 2020. 28. Article no. 101017. DOI: 10.1016/j.jobe.2019.101017

Information about the authors:

Eanas Hasan,
E-mail: ean20e1010@uoanbar.edu.iq

Muayad Al-Sharrad,
ORCID: https://orcid.org/0000-0001-6180-8837
E-mail: muayad.alsharrad@uoanbar.edu.iq

Received 06.12.2022. Approved after reviewing 15.09.2023. Accepted 15.09.2023.